COHERENT INTERACTION OF ATOMS AND MOLECULES WITH LASER RADIATION – MATHEMATICAL PROBLEMS IN MODELING COHERENT EXCITATION

Dr.Mārcis Auziņš, Dr.Linards Kalvāns, Dr. Florian Helmuth Gahbauer,
MSc. Iļja Feščenko, BSc. Agris Špīss

1. Fundamental principles of modeling coherent interaction of atom with laser radiation

To describe the atoms' (hereinafter this term refers both to atoms and molecules) coherence, the atomic density matrix *p* is used; its changes in time are described by Liouville or optical Bloch equations:

$$i\hbar = \frac{\partial \rho}{\partial t} = [\hat{H}, \rho] + i\hbar \hat{R} \rho,$$

(1)

where $\hat{H}$ denotes the Hamilton operators of the system, whose atoms, simultaneously interact with electromagnetic (laser) radiation and external magnetic field, thus the Hamiltonian consists of three parts:

$$\hat{H} = \hat{H}_0 + \hat{H}_B - \vec{d} \cdot \vec{E}(t).$$

(2)

The first term in the expression (2) describes the energy states of an unperturbed atom, which depend on the internal structure of the atom; the second term describes the atom's interaction with the external field, the third – atom's interaction with the electromagnetic radiation in dipole approximation.

The operator $\hat{R}$ in the expression (1) describes the relaxation of atoms due to both spontaneous decay (coherent relaxation) and atoms entering and leaving the region of interaction (incoherent relaxation).

Applying rotating wave approximation, decorrelation of the stochastic and time-dependent equations, as well as a formal averaging over stochastic phase in time, by using either the phase fluctuation or diffusion model, from the optical Bloch equations it is possible to obtain the rate equations for the part of the density matrix describing the Zeeman coherences [Phys. Rev. A 69, 063806 (2004)]:

$$\frac{\partial \rho_{g_i g_j}}{\partial t} = \left(\Xi_{g_i e_m} + \Xi^*_{e_k g_j} \right) \sum_{e_k, e_m} d^*_{g_i e_k} d_{e_m g_j} \rho_{e_k e_m} - \sum_{e_k, g_m} \left(\Xi^*_{e_k g_j} d^*_{g_i e_k} d_{e_k g_m} \rho_{g_m g_j} + \right.$$

$$\left. + \Xi_{g_i e_k} d^*_{g_m e_k} d_{e_k g_j} \rho_{g_i g_m} \right) - i \omega \rho_{g_i g_j} + \sum_{e_k e_l} \Gamma^{e_k e_l}_{g_i g_j} \rho_{e_k e_l} - \gamma_g \rho_{g_i g_j} + \lambda \delta(g_i, g_j)$$

$$(3a)$$

$$\frac{\partial \rho_{e_i e_j}}{\partial t} = \left(\Xi^*_{e_i g_m} + \Xi_{g_k e_j} \right) \sum_{g_k, g_m} d_{e_i g_k} d^*_{g_m e_j} \rho_{g_k g_m} - \sum_{g_k, e_m} \left(\Xi_{g_k e_j} d_{e_i g_k} d^*_{g_k e_m} \rho_{e_m e_j} + \right.$$

$$\left. + \Xi^*_{e_i g_k} d_{e_m g_k} d^*_{g_k e_j} \rho_{e_i e_m} \right) - i \omega \rho_{e_i e_j} - (\Gamma + \gamma_e) \rho_{e_i e_j}.$$

$$(3b)$$

Equations (3) are valid in case of stationary excitation, when it is possible to obtain their numerical solution, which describes quantum superposition, in which the external fields (electromagnetic and magnetic) prepare atoms. Basing on these results, it is possible to directly calculate the fluorescence signal, which is experimentally observable value. Typically, dependence of the signal of certain polarization on the external magnetic field, as well as on other excitation parameters, for example, intensity of the exciting electromagnetic radiation, diameter of the exciting beam of light or temperature in the cell of atomic vapor is modeled. Numerical solution of equations (3) is the density matrix of atomic state, that can be analyzed directly depicting it as the surface of angular momentum probability surface (http://budker.berkeley.edu/ADM/).

The system of equations (3) describes a density matrix for one particular atomic velocity group, which, as a result of Doppler effect, "sees" the EM radiation with frequency

$$f = f_0 + \Delta f, \tag{4}$$

where f_0 is the laser radiation frequency in the laboratory frame of reference, and $\Delta f = f_0 v_x$ – Doppler shift for atoms, which move with the velocity v_x in the direction of laser beam propagation. To take into account the Doppler effect, the system (3) is solved for all velocity groups in a particular region around the average value $\overline{v_x} = 0$ (a typical choice for a region is $\pm 2\sigma$) and the weighted average value of the solutions is obtained, taking into account the statistical weight of each speed group. A numerical solving of the equation system is implemented in software *steady* (see the documentation of software *steady*), which has been written in programming language *C++* and uses such open source libraries as *GSL (GNU Scientific Library), UMFPACK (Unsymmetric Multifrontal sparse lu Factorization PACKage)* and *BLAS (Basic Linear Algebra Subprograms)*. The modifications of the software *steady* are applicable to various physical systems and can be operated in computers with *Linux* operational system.

2. Modeling of coherent excitation in an extremely thin cell of atomic vapor

The applicability of the described theoretical model has been previously well tested at the excitation of the D_1 line of alkali metals (Figure 1.) in a „normal" atomic vapor cell [Phys. Rev. A 78, 013417 (2008), Phys. Rev. A 79, 053404 (2009)]. In an extremely thin cell, unlike the „normal" one, the atoms have less space to move in a direction parallel to the laser beam, and thereby the Doppler effect is significantly decreased [Opt. Comm 200, 201 (2001)], at the same time the rate of incoherent relaxation significantly increases, and additional relaxation of excited state appears, as

all atoms are located close to cell's walls and through interaction with it, the relaxation of atoms takes place.
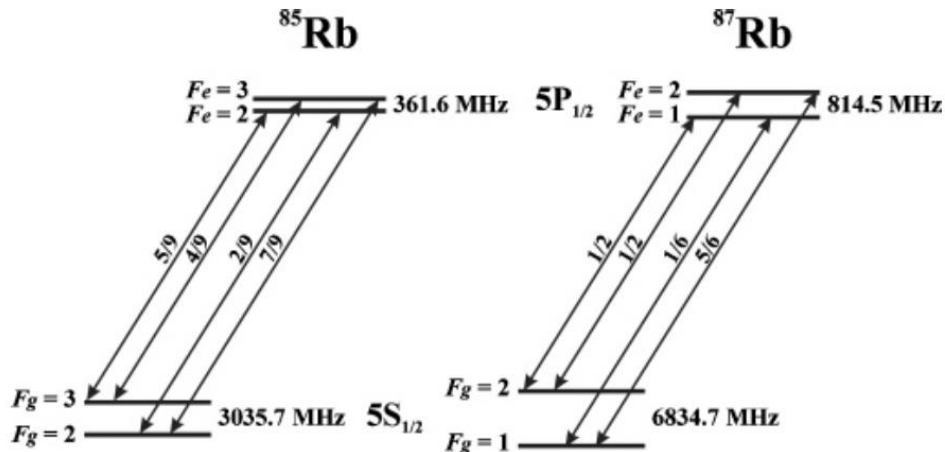

Figure1. Hyperfine level structure and allowed transitions of the D_1 spectral line of Rubidium.

To understand and evaluate the influence of these processes on the interaction between atoms and electromagnetic radiation in the presence of external magnetic field, an experiment was conducted, and the results were compared to the results of the theoretical modeling.

During the experiment the magneto-optical resonances observed at various hyperfine transitions of the D_1 spectral line of Rubidium atoms enclosed in an extremely thin cell were registered. The magneto-optical resonance is the term for resonance type changes in the fluorescence intensity, which is registered as a function of magnetic field. Magneto-optical resonances can be observed at such magnetic field values, at which two or more atomic energy levels are degenerate. In the simplest case, it is true when there is no magnetic field: $B = 0$, when the so-called *zero resonances* are formed, which were studied in the extremely thin cell.

Evaluation of theoretical model's unclear parameters (rate of the incoherent relaxation) was implemented empirically, through analysing experimentally obtained spectra, in which a fluorescence signal was registered as a function of the excitation frequency (Figure 2).
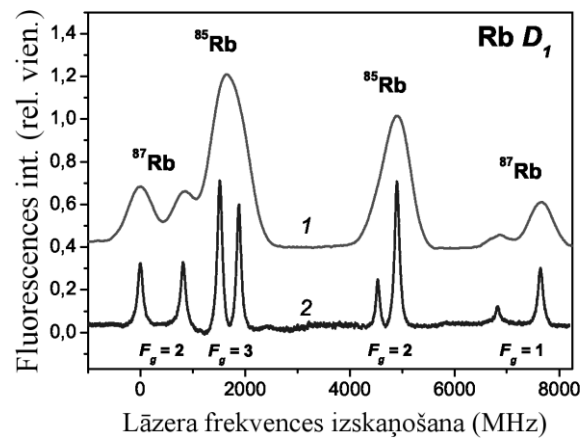

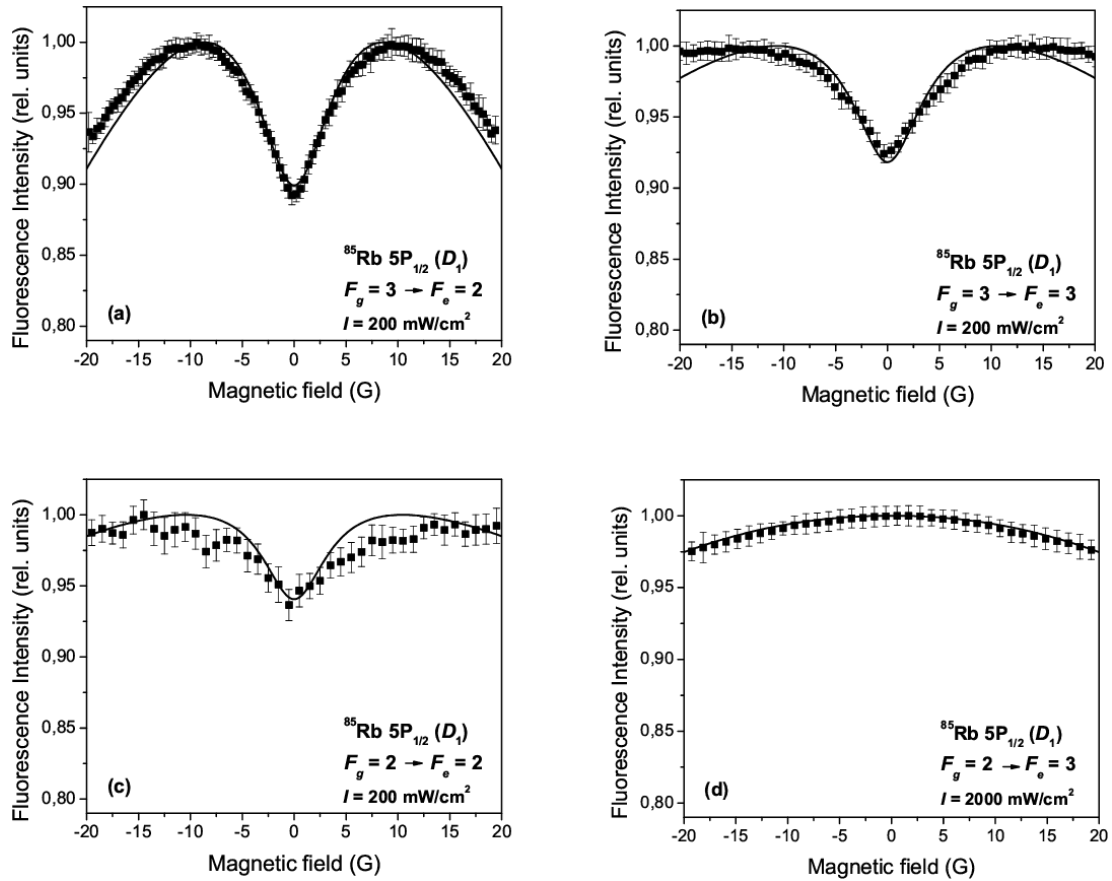Figure 2. Fluorescence excitation spectra of atomic Rubidium in an ordinary (1) and extremely thin cell (2)

Figure 3. Experimentally registered and theoretically modeled magneto-optical resonance profiles for 4 hyperfine components of the D_1 line of ^{85}Rb isotope

In this spectrum each spectral line is described by a Voigt profile, whose Gaussian part is determined by the Doppler broadening, but the Lorentzian part − by the natural line width, the collisional broadening and the interaction between atoms and cell walls. Since the natural width of spectral lines for the reviewed system is well-known and the collisional broadening can be estimated rather well, using the excitation spectrum (Figure 2) the evaluation of relaxation, which takes place when atoms interact with the walls of the cell, is also possible. The evaluation procedure in greater detail has been described in the publication [1].

Employing on the evaluated parameters of the theoretical model, the results of numerical modeling were obtained, which describe the experimental results rather well in wide range of the excitation power densities for various hyperfine components and different Rubidium isotopes at a wide region of magnetic field (±30 G) (Figures 3, 4 [1]).
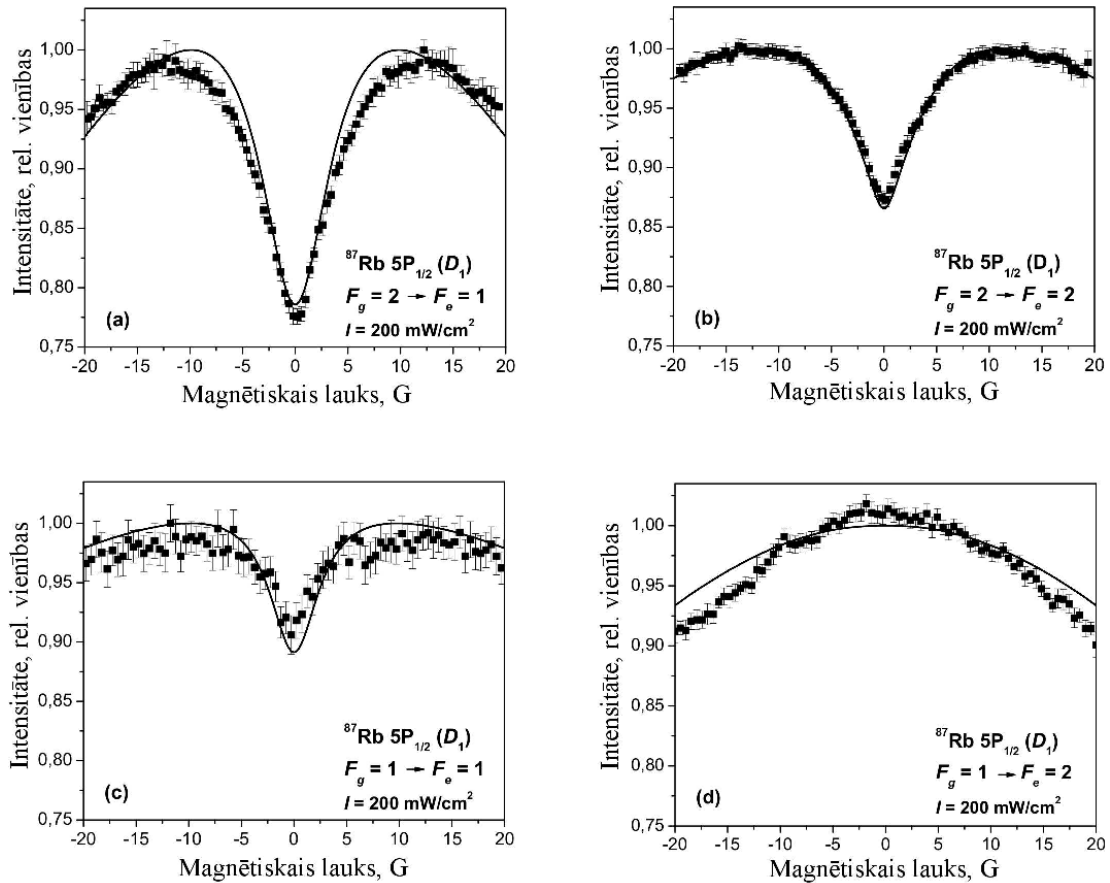
Figure 4. Experimentally registered and theoretically modeled magneto-optical resonance profiles for 4 hyperfine components of the D_1 line of [85]Rb isotope

Magneto-optical resonances are suitable for high precision measurements of magnetic field. In the extremely thin cell these resonances correspond to a magnetic field located in a very narrow sector of the space, opening up an opportunity for measurement of magnetic field gradient with spatial resolution up to $1 \mu m$.

3. Modeling of coherent excitation and coherence transfer at cascade type atomic transitions

In cascade type transitions the atoms are excited to a state, between which and the ground state several more energy levels can be encountered, and the atom can return to the ground state via a number of different transitions (Figure 5.).
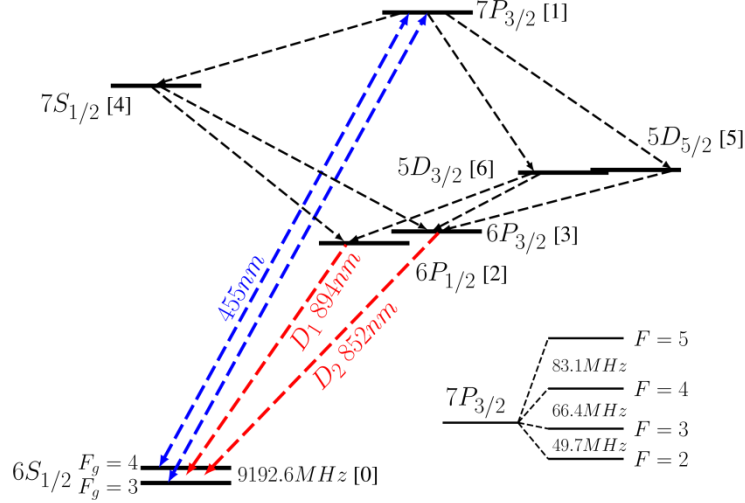

Figure 5. Cascade type transitions from Cesium $7P_{3/2}$ excited state

In the reviewed system Cesium atoms from the ground state $6S_{1/2}$ are excited to the state $7P_{3/2}$ from which they by disintegration through different transitions return to the ground state. The experiment registers both direct (455 nm) and indirect (852 and 894 nm) fluorescence and its dependence on the magnetic field.

When developing a mathematical model for such physical system, it must be taken into account that, unlike in the system (3) there are 7, not 2 distinct states which must be taken into account, therefore the system of equations to be solved is as follows [2]:

$$
\begin{aligned}
\frac{\partial \rho^{[0]}_{g_i g_j}}{\partial t} =\ & -i\omega_{g_i g_j}\rho^{[0]}_{g_i g_j} - \gamma\rho^{[0]}_{g_i g_j} + \left(\sum_{e_k e_m} \Gamma^{[1]e_k e_m}_{[0]g_i g_j}\rho^{[1]}_{e_k e_m} + \sum_{e_k e_m} \Gamma^{[2]e_k e_m}_{[0]g_i g_j}\rho^{[2]}_{e_k e_m} + \sum_{e_k e_m} \Gamma^{[3]e_k e_m}_{[0]g_i g_j}\rho^{[3]}_{e_k e_m} \right) \\
& + \frac{|\varepsilon_\varpi|^2}{\hbar^2} \sum_{e_k,e_m} \left(\frac{1}{\Gamma_R + i\Delta_{e_m g_i}} + \frac{1}{\Gamma_R - i\Delta_{e_k g_j}} \right) d^*_{g_i e_k} d_{e_m g_j}\rho^{[1]}_{e_k e_m} \\
& - \frac{|\varepsilon_\varpi|^2}{\hbar^2} \sum_{e_k,g_m} \left(\frac{1}{\Gamma_R - i\Delta_{e_k g_j}} d^*_{g_i e_k} d_{e_k g_m}\rho^{[0]}_{g_m g_j} + \frac{1}{\Gamma_R + i\Delta_{e_k g_i}} d^*_{g_m e_k} d_{e_k g_j}\rho^{[0]}_{g_i g_m} \right) \\
& + \lambda\delta\left(g_i, g_j \right)
\end{aligned}
\tag{5}
$$

$$\frac{\partial \rho_{e_i e_j}^{[1]}}{\partial t} = -i\omega_{e_i e_j} \rho_{e_i e_j}^{[1]} - \left(\gamma + \Gamma^{[1]}\right) \rho_{e_i e_j}^{[1]} + (0)$$
$$+ \frac{|\varepsilon_{\varpi}|^2}{\hbar^2} \sum_{g_k, g_m} \left(\frac{1}{\Gamma_R - i\Delta_{e_i g_m}} + \frac{1}{\Gamma_R + i\Delta_{e_j g_k}} \right) d_{e_i g_k} d_{g_m e_j}^* \rho_{g_k g_m}^{[0]}$$
$$- \frac{|\varepsilon_{\varpi}|^2}{\hbar^2} \sum_{g_k, e_m} \left(\frac{1}{\Gamma_R + i\Delta_{e_j g_k}} d_{e_i g_k} d_{g_k e_m}^* \rho_{e_m e_j}^{[1]} + \frac{1}{\Gamma_R - i\Delta_{e_i g_k}} d_{e_m g_k} d_{g_k e_j}^* \rho_{e_i e_m}^{[1]} \right), \tag{6}$$

$$\frac{\partial \rho_{f_i f_j}^{[2]}}{\partial t} = -i\omega_{f_i f_j} \rho_{f_i f_j}^{[2]} - \left(\gamma + \Gamma^{[2]}\right) \rho_{f_i f_j}^{[2]}$$
$$+ \left(\sum_{e_k e_m} \Gamma_{[2]f_i f_j}^{[4]e_k e_m} \rho_{e_k e_m}^{[4]} + \sum_{e_k e_m} \Gamma_{[2]f_i f_j}^{[6]e_k e_m} \rho_{e_k e_m}^{[6]} \right), \tag{7}$$

$$\frac{\partial \rho_{f_i f_j}^{[3]}}{\partial t} = -i\omega_{f_i f_j} \rho_{f_i f_j}^{[3]} - \left(\gamma + \Gamma^{[3]}\right) \rho_{f_i f_j}^{[3]}$$
$$+ \left(\sum_{e_k e_m} \Gamma_{[3]f_i f_j}^{[4]e_k e_m} \rho_{e_k e_m}^{[4]} + \sum_{e_k e_m} \Gamma_{[3]f_i f_j}^{[5]e_k e_m} \rho_{e_k e_m}^{[5]} + \sum_{e_k e_m} \Gamma_{f_i f_j}^{[6]e_k e_m} \rho_{e_k e_m}^{[6]} \right), \tag{8}$$

$$\frac{\partial \rho_{f_i f_j}^{[4]}}{\partial t} = -i\omega_{f_i f_j} \rho_{f_i f_j}^{[4]} - \left(\gamma + \Gamma^{[4]}\right) \rho_{f_i f_j}^{[4]} + \sum_{e_k e_m} \Gamma_{[4]f_i f_j}^{[1]e_k e_m} \rho_{e_k e_m}^{[1]}, \tag{9}$$

$$\frac{\partial \rho_{f_i f_j}^{[5]}}{\partial t} = -i\omega_{f_i f_j} \rho_{f_i f_j}^{[5]} - \left(\gamma + \Gamma^{[5]}\right) \rho_{f_i f_j}^{[5]} + \sum_{e_k e_m} \Gamma_{[5]f_i f_j}^{[1]e_k e_m} \rho_{e_k e_m}^{[1]}, \tag{10}$$

$$\frac{\partial \rho_{f_i f_j}^{[6]}}{\partial t} = -i\omega_{f_i f_j} \rho_{f_i f_j}^{[6]} - \left(\gamma + \Gamma^{[6]}\right) \rho_{f_i f_j}^{[6]} + \sum_{e_k e_m} \Gamma_{[6]f_i f_j}^{[1]e_k e_m} \rho_{e_k e_m}^{[1]}. \tag{11}$$

Each of the equations (5-11) describes the evolution of the demonstrated atomic states in time; all equations together form a linear system of differential equations, which can be solved for stationary state, when the left hand side of all the equations are set to zero.

A numerical solution of system (5)-(11) required extensive resources; therefore it was very important to evaluate the initial parameters very carefully. Similarly to the system (3), the current system was also averaged in Doppler profile.
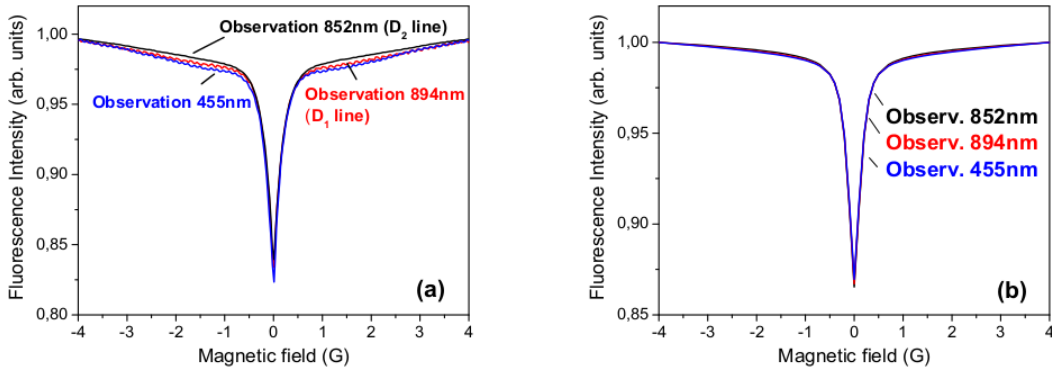

Figure 6. Three components of the fluorescence observed in the cascading decay after the excitation of Cs $6P_{1/2}$ ($F_g = 3$) --> $7P_{3/2}$. Experimental results (to the left) and theoretical model results (to the right) [2]

The fluorescence signals of the cascade transitions excited from the different hyperfine levels of the ground state for all three observed wavelengths are pictured in Figures 6 and 7.
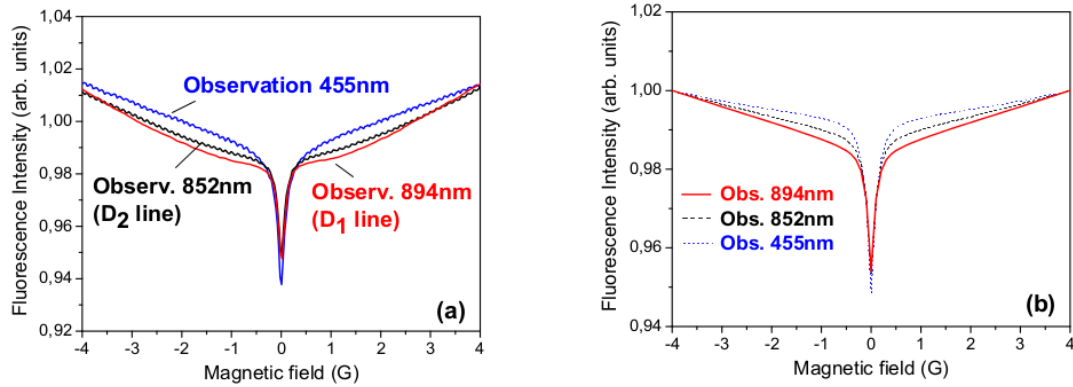
Figure 7. Three components of the fluorescence observed in the cascading decay after the excitation of Cs $6P_{1/2}$ ($F_g = 4$) --> $7P_{3/2}$. Experimental results (to the left) and theoretical model results (to the right) [2]

The research of cascade pathways testify, that laser radiation induced coherences in excited states are effectively transferred to lower states, which do not directly interact with the exciting radiation. Thereby it is possible to optically polarize isolated atomic states and to avoid various undesirable side-effects in the process of polarization. The results of theoretical modeling testify that also in case of very complicated physical systems the theoretical model provides a satisfactory description, regardless of the fact that it is not possible to carry out the parameter matching due to the limited computer resources.

4. Modeling of coherent excitation in molecules with a large angular momentum quantum number

Energy structure of diatomic (and multiatomic) molecules is significantly more complex than that of separate atoms. The energy structure is divided in three levels:
1. Electronic energy levels;
2. Vibrational energy levels;
3. Rotational energy levels.

Each subsequent group's characteristic distances among different energy levels are at least by one order smaller – each electronic level contains a large number of vibrational levels, and each of the vibrational levels – a large number of rotational levels. Atomic energy, in turn, can be described only with the electronic energy levels, because the vibrations and rotation around the center of symmetry of the internuclear bonds cannot take place in atoms. The electronic levels are described by orbital and full electronic or atom angular momentum quantum numbers which are typically rather small (<10), while the vibrational and rotational quantum numbers can reach significantly higher values. Taking into account all the aforementioned, it can be concluded that in case of molecules the mathematical description of energy levels and the coherent processes which take place therein, are significantly more complex than in the case of atoms.

Therefore, when studying the coherent processes in molecules it is endeavored to use systems, which are physically simpler – it is rather typical to study diatomic molecules of alkali metals. In mathematical modeling it is carefully weighed, which molecular energy structure's qualities it is necessary to take into account and which can be forgone, without losing the ability to describe the real physical system.

In the framework of the project a study of the magneto-optical resonances observed in K_2 molecules at energy states with large rotational quantum number values, was implemented. The transition of K_2 molecule between electronic levels $X_1\Sigma_g^+\rightarrow B^1\Pi_u$, was chosen as a physical system of research, observing the fluorescence to the same electronic level, the vibrational number of the ground state was chosen v''=0, of the excited state v'=0, and fluorescence was observed to the level v_1''=3. Rotational quantum numbers were chosen J''=99$\rightarrow$J'=99$\rightarrow$$J_1$''=99 (Q-type transition) and J''=105$\rightarrow$J'=106$\rightarrow$$J_1$''=107 (R-type transition). When developing a mathematical model it was presumed that the contiguous rotational levels are located sufficiently distant each to other, in order to avoid influence of the neighboring levels neither as a result of Doppler effect, nor as a result of level mixing, which does not apply to rotational levels. Taking into account these considerations, diatomic molecules could be described in basis$|\xi, J_i, m_J\rangle$, where J_i is the rotational quantum number of the ground or excited state and m_J – the corresponding magnetic quantum number or projection of rotation momentum on quantization axis, and ξ describes all the remaining quantum numbers, which in the framework of chosen transition remain unchanged. When describing a molecular system in such basis, it is possible to attribute to it a system of differential equations (3), which can be transformed in a system of linear equations, presuming that excitation has entered a stationary state and the time derivatives of the density matrix elements can be equated to zero.

However, the assignment to solve this system of linear equations is not particularly simple, as the system is composed of altogether (2*J'' + 1)(2*J' + 1) equations, which, on the whole, make approximately 40 000 equations for description of the chosen physical system. Considering that the solutions of the equations are complex numbers, the actual number of unknown values is even 2 times greater. For solving this type of systems directly, very powerful computers are required and it is time-consuming. The numerical task can be simplified by taking into account the fact that the in coefficients' matrix corresponding to the linear system of equations most elements are equal to zero – in the described physical system the proportion of non-zero elements in the matrix is approximately 10^{-4}. For the operations with such partially filled matrix it is possible to use special algorithms, which take into account only the elements differing from zero.
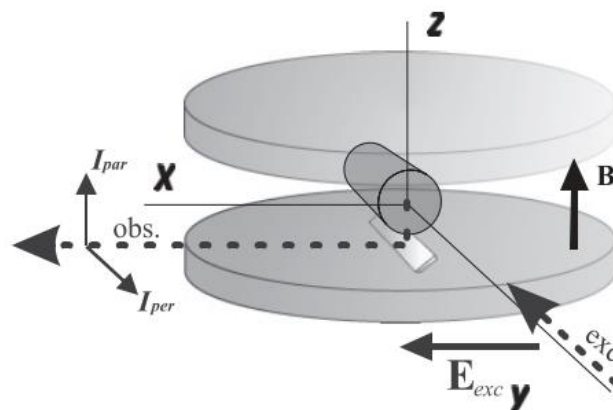

Figure 8. Excitation and observation geometry, observing the magneto-optical resonances in K_2 molecule [3]

First of all, the matrix must be stored in a special form, indicating the indexes and values of the elements different from zero, and not all the values sequentially, thereby for storing one element (different from zero) a three times larger memory is used, however, taking into account the fill of the matrix in the task under consideration,

$3*10^{-4}$ of that memory, which would otherwise have been used with a coefficient matrix in the traditional form, is being occupied. An open spource *C++* library *UMFPACK (Unsymmetric Multifrontal sparse lu Factorization PACKage)* [ACMTrans.Math. Softw. 30, 165 (2004)] is used to treat these matrices. When solving a linear equation system, which is written in form $A\mathbf{x} = \mathbf{b}$, it is necessary to diagonalize the matrix A, which is the previously described, partially filled matrix of coefficients. The library used for the numerical modeling divides this matrix into sub-matrices, which have been aligned along the main diagonal, and in each subsequent step carrying out this operation with formerly created sub-matrices, until their size decreases to one element and the initial matrix is diagonalized. During the work with the numerical modeling it was concluded that the use of UMFPACK algorithm becomes justified (faster than diagonalization of a full matrix) in a situation when the fill of the matrix is about 10^{-1}, which becomes effective at J ≈ 10. Therewith the numerical modeling was implemented by diagonalizing the coefficient matrix of linear equations' system, applying UMFPACK algorithm. The numerical model solved in this manner allowed implementing the necessary calculations with regular computers in order to model the experimental results. During the experiments the magneto-optical resonances were observed in the adjacency of magnetic field B = 0, changing the field within the limits from 0 to10 000 gauss. The obtained results of modeling correspond well to those registered during the experiment, the dark resonance is being observed with the characteristic width of several hundred gauss both in separate fluorescence components with orthogonal polarization (see Figure 8), and the degree of polarization of the fluorescence (Figures 9 and 11).
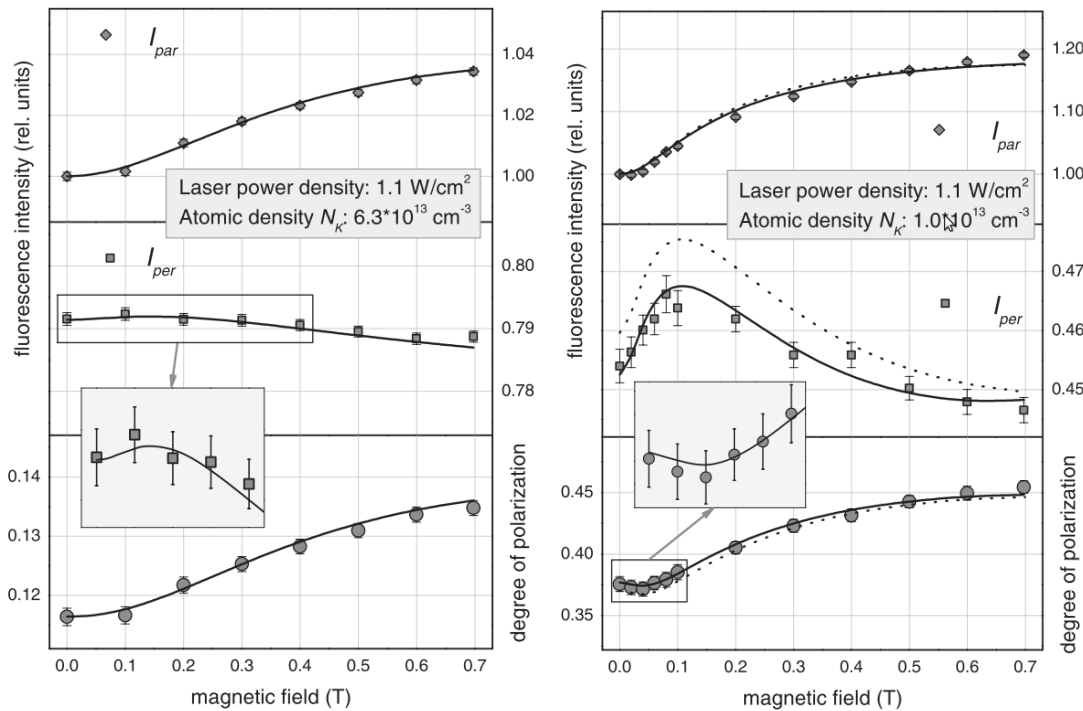

Figure 9. Magneto-optical resonances registered experimentally (dots) and modeled theoretically in K_2 molecule. To the left - R transition, to the right - Q transition [3]
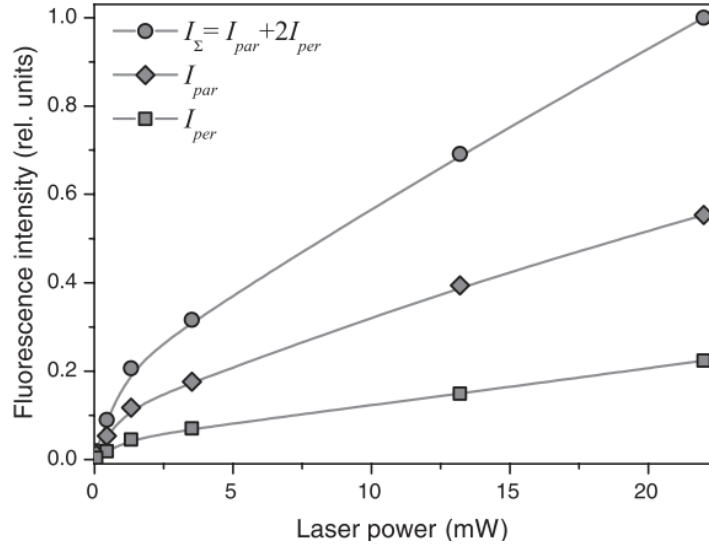
Figure 10. Dependence of the full fluorescence on the laser power density, experimental data.
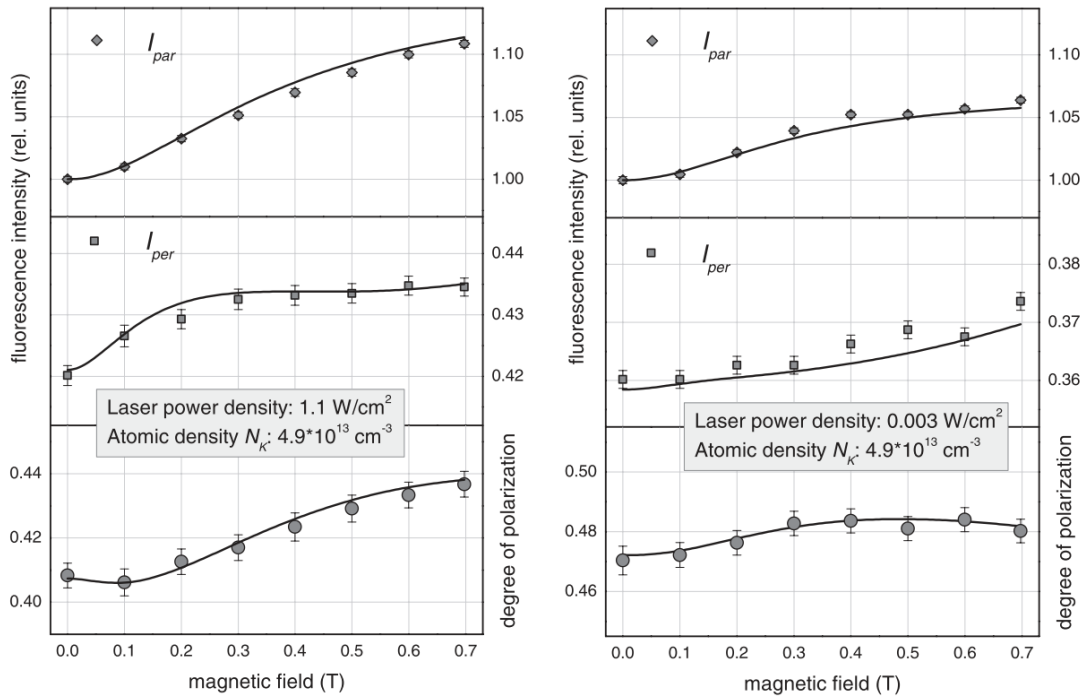

Figure 11. Magneto-optical resonances registered experimentally (dots) and modeled theoretically in K_2 molecule. Q – type excitation, lower atom concentration than in Figure 8. To the left – high laser power density, to the right – low laser power density [3]

The theoretical model provides a very good description of experimental results and can be successfully applied for the description of systems with a large angular momentum.

It must be added that in the process of modeling, when working with magneto-optical resonances, which have been obtained at different exciting radiation's power densities, Rabi frequencies must be used, which are obtained by different algorithms, illustrated in Figure 10. It can be observed, that by increasing the density of exciting

power, the fluorescence at low powers grows according to one linear relation, however, when the powers are high, according to another, thereby testifying that that a certain fluorescence saturation takes place and increasingly greater importance is attached to the relatively low power regions at the wings of laser beam profile.

5. Tests of the mathematical model for coherent excitation in atomic processes of high sensitivity

In typical application of magneto-optical resonances for measurement of magnetic field or magnetometry it is most important that the resonances which are narrow and have a large contrast, which is usually characteristic for dark resonances. The bright resonances, which have a weak contrast, are considered to be an interesting phenomenon; however they as yet have no practical application. However, it does not mean that these weak bright resonances are insignificant in the research process. Particularly the processes of this kind – weak and sensitive to the experimental conditions are especially important in the testing process of the theoretical model, because it can clearly show the ability of the model to quantitatively describe of the physical reality.
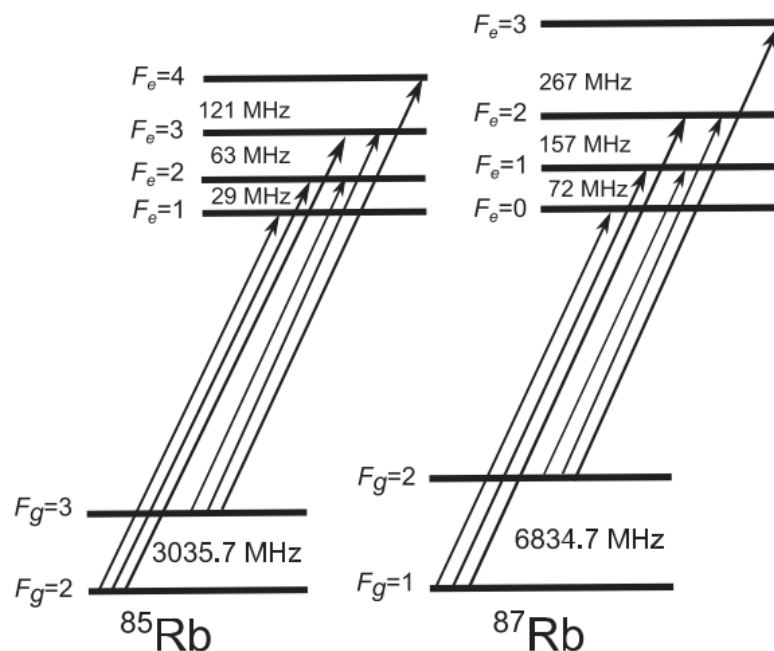

Figure 12. Hyperfine level structure and transitions of the D_2 line of rubidium.

An interesting example of such bright resonances can be observed at the hyperfine components of the D_2 spectral line of Rubidium (Figure 12) $F_g = 2 \rightarrow F_e = 3$ (I; [87]Rb) or $F_g = 3 \rightarrow F_e = 4$ (II; [85]Rb). These transitions according to their general structure $F_g \rightarrow F_e = F_g + 1$ correspond to the bright resonances, however, studying them in the atomic vapor cell, as a result of the Doppler effect the particular hyperfine components are affected by others located nearby in terms of energy. The neighboring components give raise to a dark resonance with a larger contrast. Therefore the transitions (I) and (II) are expressed very weakly and sensitive toward such conditions as insignificant changes in exciting laser radiation frequency, as well as in the excitation power density. The theoretical modeling, using the theoretical model,

which is described by system (3), was implemented simultaneously with the experimental study of the magneto-optical resonances observed in the mentioned transitions. The results of the modeling testified that at low of excitation power densities in both transitions a bright resonance is expected with a low (< 0,1%) contrast, which, when the power density is increased, turns into a dark resonance. The initial experimental results did not give an evidence of these bright resonances. However, working with the experimental equipment, deficiencies were detected, and after their correction, the bright resonances predicted by the theoretical model were observed. Additionally, the change of the resonance sign (from light to dark) was observed in detail by increasing the density of exciting power and fully confirming the results of theoretical model (Figures 13 and 14).
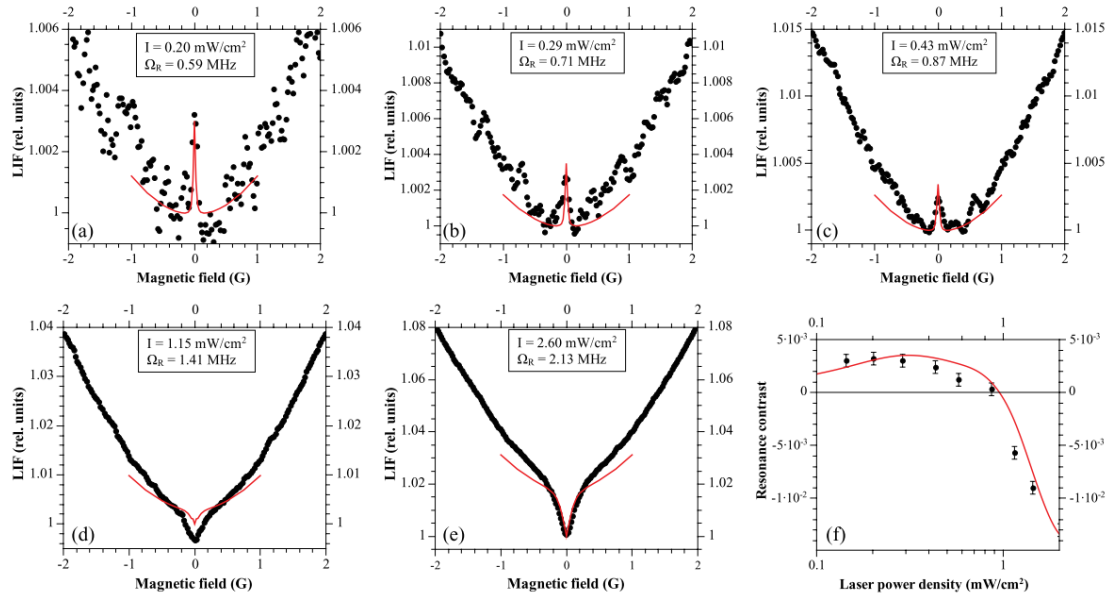

Figure 13. ^{85}Rb D2 lines $F_g = 3 \rightarrow F_e = 4$ the dependence of magneto-optical resonances (observed at a hyperfine transition) on the exciting radiation power density (a-e) and dependence of the resonance contrast on the power density (f) [4]

Figure 14. ^{87}Rb D2 lines $F_g = 2 \rightarrow F_e = 3$ the dependence of magneto-optical resonances (observed at a hyperfine transition) on the exciting radiation power density (a-e) and dependence of the resonance contrast on the power density (f) [4]
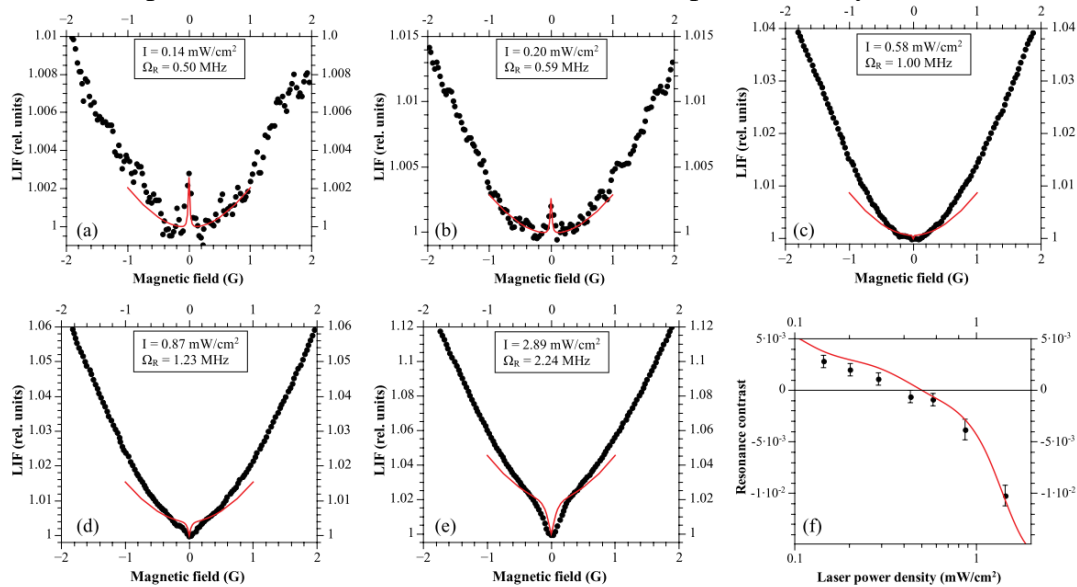
During the ensuing course of study the theoretical model's information about coherent states of atom was used to study the basis for the change of resonance sign. The initial hypothesis about the overlapping of the hyperfine transitions caused by the Doppler effect were rejected by the model results (Figure 15, to the left). It was recognized that the effect is geometric by nature – by observing the resonance in full fluorescence, which is formed by the sum of three orthogonal polarization components ($I_x + I_y + I_z$), model does not imply the change of resonance sign. However, in experimentally implementable observation of fluorescence in one direction, it is formed by two components ($I_x + I_y$) and for this sum a resonance sign change can be observed (Figure 15, to the right), testifying that under the influence of magnetic field the angular momentum precession takes place in the excited state.
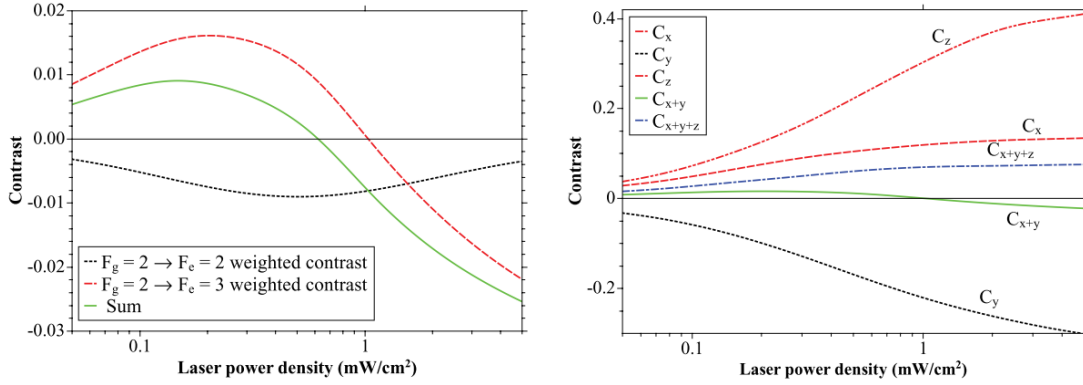

Figure 15. ^{87}Rb D2 lines $F_g = 2 \rightarrow F_e = 3$ the dependence of the contrast of magneto-optical resonances (observed in hyperfine transitions) on the power density of the exciting radiation. The contrast observed for various velocity groups (to the left); the contrast observed in various fluorescence components (to the right) [4]

These results confirm the capacity of the atom's coherent excitation mathematical models both to quantitatively describe the physical reality and to describe an easily comprehensible explanation to processes taking place in an atomic environment.

6. Modeling of level crossing signals at non-zero magnetic field in atomic vapor cell at Rubidium D$_2$ excitation

Previously described magneto-optical resonances in all cases were the so-called zero resonances, when signals were observed at zero magnetic field, when magnetic sub-levels with equal full atomic angular momentum F or J are degenerated. The energy structure changes in magnetic field are described by operator $\widehat{H}_B$ in (3), which can be written explicitly as

$$H_B = \frac{\mu_B}{\hbar} \left(g_J \mathbf{J} + g_I \mathbf{I} \right) \cdot \mathbf{B}, \tag{12}$$

where μ_B denotes the Bohr magneton, $\mathbf{J}$ and $\mathbf{I}$ – respectively the total electronic angular momentum and spin of the atomic nucleus, the sum of which is the full atomic angular momentum $\mathbf{F} = \mathbf{J} + \mathbf{I}$, g_J and g_I are the respective Landé factors. The Hamiltonian operator (12) consists of interaction matrices for fixed angular momentum projection on the quantization axes $m_F = m_J + m_I$, and can be written in terms of Vigner $3j$ and $6j$ symbols:

$$\mathbf{J} \cdot \mathbf{B} = (-1)^{J+I+F_i+F_k-m_F+1} \sqrt{(2F_i + 1)(2F_k + 1)J(J + 1)(2J + 1)} \cdot \tag{13}$$
$$\begin{pmatrix} F_i & 1 & F_k \\ -m_f & 0 & m_f \end{pmatrix} \cdot \begin{Bmatrix} J & F_i & I \\ -F_k & J & 1 \end{Bmatrix};$$

$$\mathbf{I} \cdot \mathbf{B} = (-1)^{J+I+F_i+F_k-m_F+1}\sqrt{(2F_i+1)(2F_k+1)I(I+1)(2I+1)} \cdot \quad (14)$$

$$\begin{pmatrix} F_i & 1 & F_k \\ -m_f & 0 & m_f \end{pmatrix} \cdot \begin{Bmatrix} I & F_i & L \\ -F_k & I & 1 \end{Bmatrix},$$

where $\begin{pmatrix} . & . & . \\ . & . & . \end{pmatrix}$ is *3j*, and $\begin{Bmatrix} . & . & . \\ . & . & . \end{Bmatrix}$ – *6j* symbol, L is the electronic orbital angular momentum quantum number. Expanding the magnetic field and atomic internal energy interaction's Hamiltonian operator (12), as a matrix in accordance with (13) and (14) and solving the eigenvalue problem for this matrix yields the eigenvalues for magnetic sublevel energies (Figures 16 and 17). It can be observed that there are relatively many magnetic field values, at which the energies of different magnetic sublevels match.
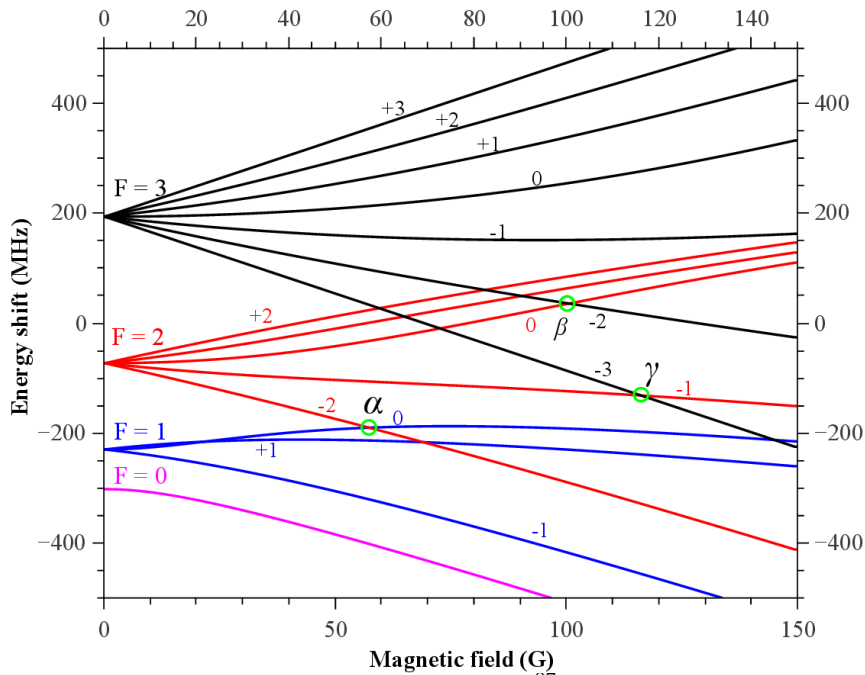

Figure 16. Level splitting of hyperfine structure in ^{87}Rb state $5P_{3/2}$.
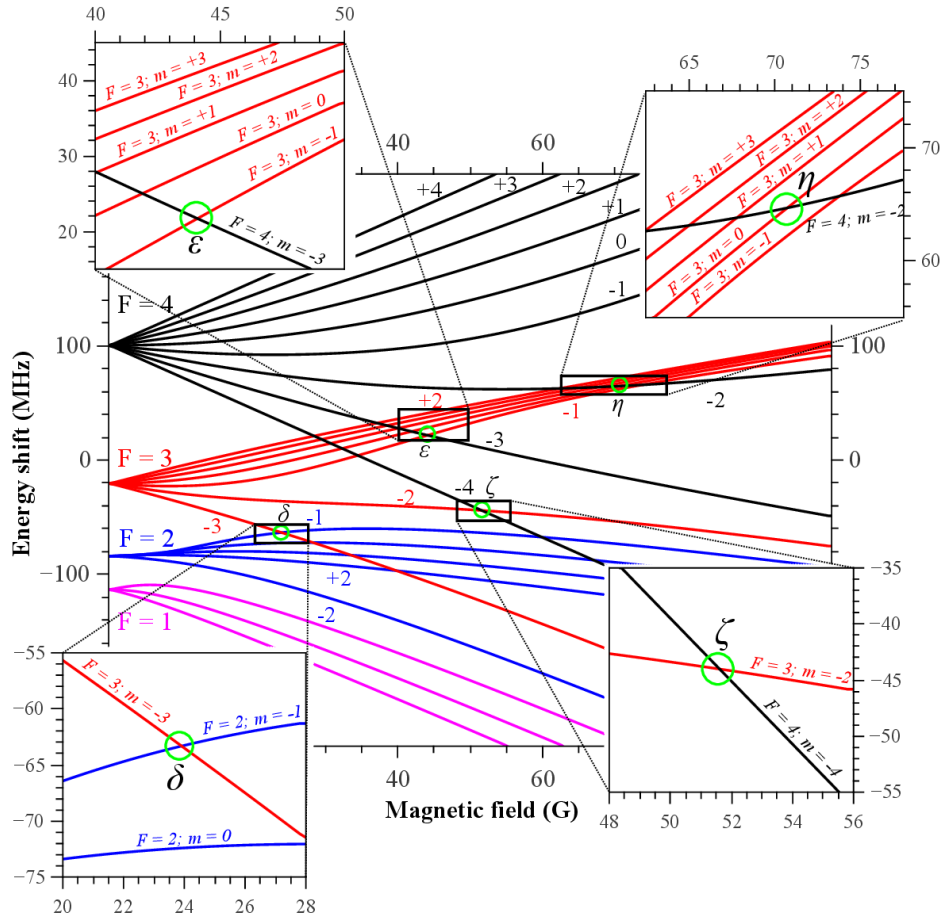
Figure 17. Level splitting of hyperfine structure in ^{87}Rb state 5P$_{3/2}$.

However, the level crossing signals are not observed in all of these crossing points. The basic condition necessary for it to happen is the capacity of one photon of the exciting electromagnetic radiation to connect both these sublevels with one and the same level of the ground state. It is possible if the following condition is fulfilled:

$$\Delta m \leq 2. \qquad (15)$$

Thereby all the crossing points in which the level crossing resonance signals can be observed can be divided into 3 groups:

1. $\Delta m = 0$: such crossing points do not exist;
2. $\Delta m = 1$: such crossing points can be observed in the geometry of excitation, where the angle between the direction of the exciting radiation polarization axis and the vector of magnetic field induction is not 0° or 90°;
3. $\Delta m = 1$: such crossing points can be observed in geometry, where the angle between the direction of the exciting radiation polarization direction and the vector of magnetic field induction is 90°;

The most pronounced resonances can be observed for the crossing points of the 3rd type, which were chosen for research in the experiments of University of Latvia Laser Centre. These crossing points in Figures 16 and 17 are denoted with the letters of Greek alphabet. The positions of these resonances in magnetic field are determined by hyperfine structure splitting and similar resonances historically have been used for determination of atomic constants. If detailed information about the atomic energy structure is known, these resonances can be used for calibration of the magnetic field as markers of field values, while measuring the field in the region of a few tens of

Gauss. In the context of this procedure it is important that the resonances would be as expressed as possible, mostly for their contrast to be as high as possible.

The resonances of this type can be most easily observed in polarization of fluorescence, studying two orthogonal linearly polarized fluorescence components, one of which has a polarization parallel to that of the exciting radiation, and the observation is implemented along the direction of magnetic field induction vector.

When registering a signal it is important to set the frequency of exciting radiation as precisely as possible, so that at a particular crossing point the coherences are induced as effectively as possible. It is particularly imperative when working with ^{87}Rb isotopes, which have larger values of hyperfine structure level splitting.

Thereby the goal of the study was set to maximize the resonance contrast of the level crossing signals by accurately matching the frequency of exciting radiation to the level crossing energy, as well as to demonstrate the capacities of the theoretical model, which is based on optical Bloch equations, to provide a quantitative description of these level crossing effects.

At the outset the research work was dedicated to theoretical modeling, to determine the precise positions of crossing points and the resonance contrasts at various frequencies of exciting radiation. The result of this modeling is shown in Figure 18 for ^{87}Rb isotope. The contrast of crossing point α, depending from the laser frequency, in the excitation from the hyperfine level $F_g = 2$ of the ground state can change even four times, and in the excitation from $F_g = 1$, where it forms the most intensive resonance in the entire system investigated – almost two times. Subsequently, according to the results of theoretical modeling, it is possible to achieve a significant improvement in observation of resonances by choosing an appropriate frequency of the exciting radiation.
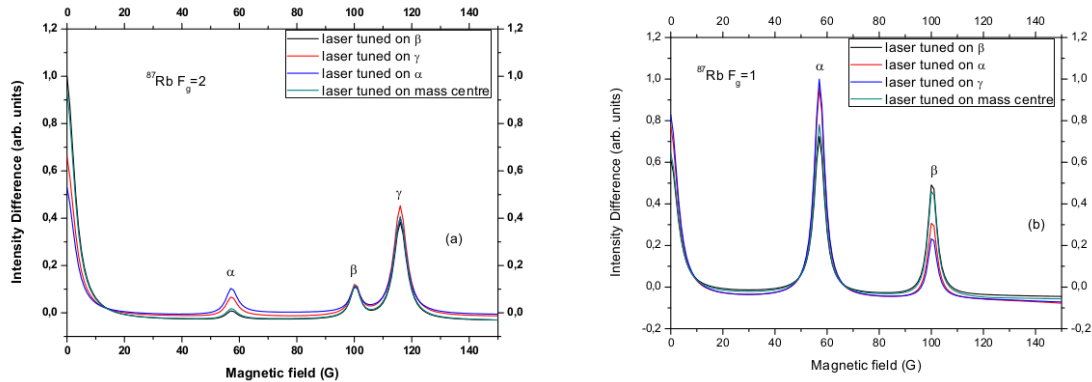

Figure 18. The resonance profiles of the level crossing observed at ^{87}Rb D$_2$ excitation, depending on the frequency of the exciting radiation

The experimental results were registered by successive observation of fluorescence at the excitation frequencies corresponding to each of the crossing points depicted in Figures 16 and 17, and also at various exciting radiation power densities. An example of these results is shown in Figure 19, where it can be seen that the theoretical model provides a very good description of the experimental signal at low power densities, and a slightly poorer – at higher laser power densities.
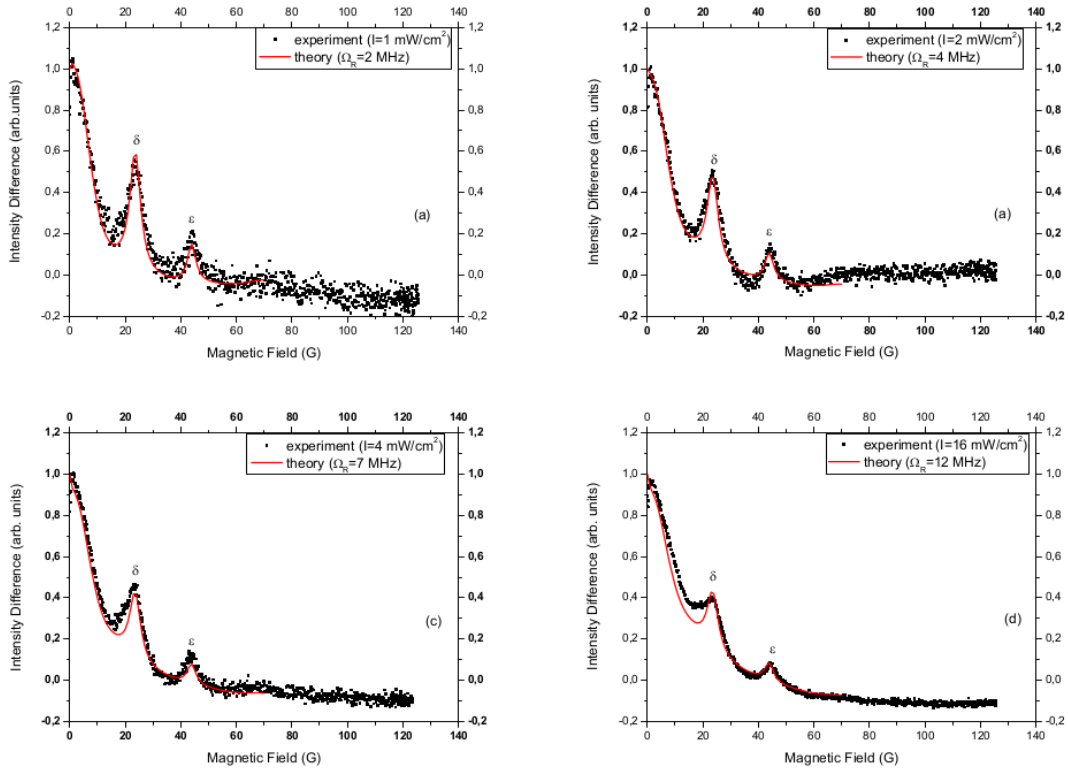
Figure 19. The dependence of the level crossing resonance signals on the excitation power density at D_2 excitation of ^{85}Rb

The dependence of the level crossing resonance signals on the frequency of the exciting radiation in ^{87}Rb atoms shown in Figure 20, gives an experimental confirmation of the results of theoretical model emphasizing the significant influence of excitation frequency on the signal contrast in these particular transitions.
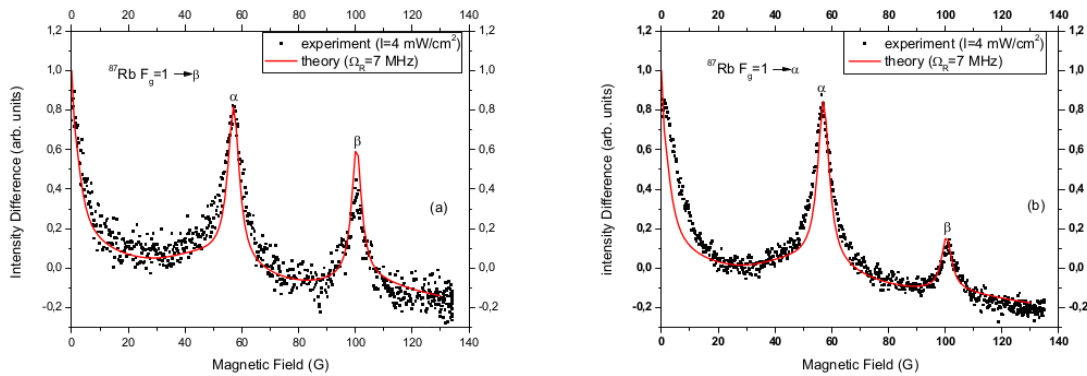

Figure 20. The dependence of the level crossing resonance signals on the excitation frequency at D_2 excitation of ^{87}Rb

Finally, in studies of level crossing signals, the opportunity was used to visualize the excited state density matrixes (Figure 21) obtained from the theoretical model. These images show that the polarized fluorescence radiation is emitted by atoms, whose angular momentum probability distribution is asymmetrical in the observation (*xy*) plane (Figure 21, (a) and (c)), and an isotropic angular momentum distribution corresponds to an isotropic fluorescence signal (Figure 21, (b)).
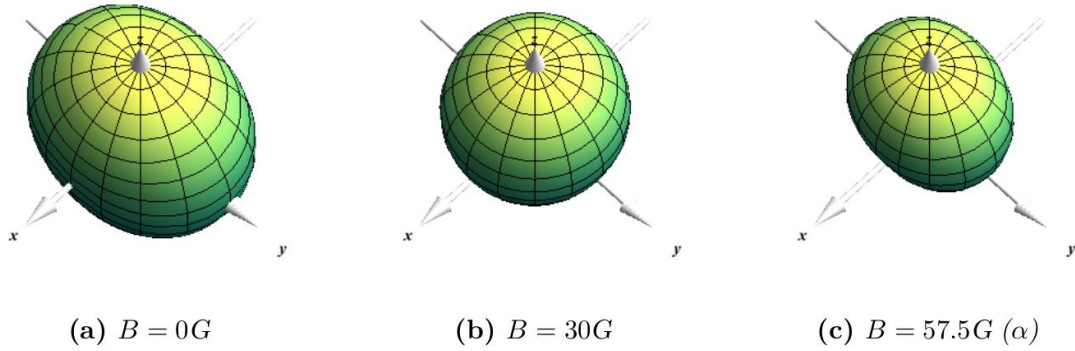
(a) $B = 0G$ (b) $B = 30G$ (c) $B = 57.5G \ (\alpha)$

Figure 21. Visualization of density matrices for D_2 excitation of ^{87}Rb at various values of the external magnetic field inductance

The results of studies of the level crossing signals for $\Delta m = 2$ are currently being summarized in a manuscript of a scientific publication [5].

A research work has commenced also regarding the $\Delta m = 1$ level crossing signals. In the framework of this study a theoretical modeling has been implemented and the experimental results registered. The most interesting results testify the possibility to simultaneously register both $\Delta m = 1$ and $\Delta m = 2$ resonances, thereby obtaining an additional point of reference for calibrating the magnetic field. The modeling results of these observations are shown in Figure 22. However, it must be admitted that for the present these results are not yet obtained in experiment, as it is technically very difficult to set up the necessary excitation geometry.
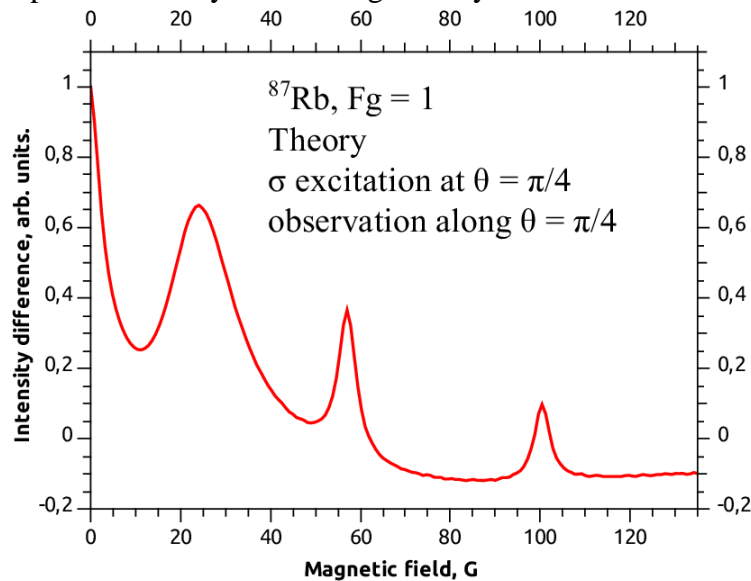

Figure 22. Level crossing signal, where the resonances $\Delta m = 1$ un $\Delta m = 2$ can be observed simultaneously

7. Other research directions

7.1. Spin squeezing

Spin squeezing is an effect in which an atom, by optical polarization, is prepared in the state of minimum uncertainty, where the atom's angular projection in a particular direction (for example, along the z axis) is maximal, and along the remaining two axis (in the xy plane) it is minimal and uncertainty in this plane is with a minimum possible value according to Heisenberg uncertainty relations, additionally the

uncertainty in the *xy* plane is isotropic. In such a situation placing the atom in an external electric field, the spin "squeezing" takes place in the *xy* plane – in a certain direction depending on electric field, the uncertainty decreases, but in a direction perpendicular to it – increases. This process can be compared to a squeezing of a circle into an ellipse [Phy. Rev. A, **85** 022125]. As a result a direction in space is obtained, where the atomic spin is determined even more precisely than in the initial minimum uncertainty state. When using the atoms to measure magnetic field it is important that their state is known as precisely as possible, thereby the measurement precision can be improved.

Taking into account that the described effect increases with the increase of the angular momentum, an appropriate physical system for implementation of it is a diatomic molecule, where very high values of rotational quantum number are possible. It was decided to implement such an experiment in a stationary excitation of NaRb molecules. In order to plan the experiment successfully, a simple theoretical model was created to describe the expected results. It is presumed in the model that the atoms are prepared in the condition of minimum uncertainty:

$$\rho'^{(P)}_{m,m'} = \delta(m, m')\delta(m, J), \tag{16}$$

where *m* is the magnetic quantum number, but J – the quantum number of the angular momentum (rotational). The density matrix (16) is rotated by $-\pi/2$ around *y* axis, so that the new quantization axis and the external electric field would be perpendicular to the direction of maximum angular momentum projection. It is presumed that the density matrix changes in time according to the optical Bloch equations (1), where the Hamilton operator is composed by the internal Hamiltonian of the atom and the interaction with the electric field as quadratic Stark effect:

$$E_m = \frac{d^2 E^2}{\hbar B_J} \cdot \frac{J(J+1) - 3m^2}{2J(J+1)(2J-1)(2J+3)}, \tag{17}$$

Where *d* is the permanent dipole momentum, E – electric field intensity, and B_J – rotational constant. Considering that the atomic relaxation operator for Bloch equations can be written as

$$\hat{R}\rho = \Omega \, \rho^{(P)} - \gamma\rho, \tag{18}$$

where the optical pumping takes place in accordance with (16) and with a rate Ω, the following stationary solution of the equation (1) is obtained:

$$\rho_{m,m'} = \frac{\Omega\rho^{(P)}}{\gamma + i\Delta E_{m,m'}}. \tag{19}$$

The density matrices obtained in this way can be used to directly calculate absorption as a function of the electric field. An example of such calculations is presented in Figure 23.
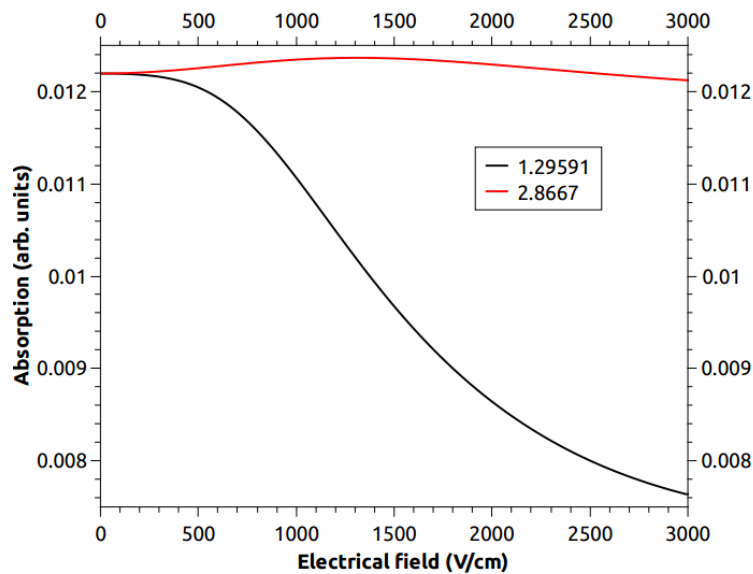
Figure 23. The absorption signal for two orthogonal excitation components depending on electric field, modeling the spin squeezing signal

The results show that the absorption increases for one of the orthogonal components, corresponding to the effect of spin squeezing, and the absorption decrease of the other component takes place because the electric field detunes the respective transitions from resonance. Currently the experiment is prepared in the University of Latvia Laser Centre, where it will be possible to test the correspondence of the modeled results to the physical reality.

7.2. NV optical centers

During the project the preparations have been completed to begin the research of the nitrogen – vacancy (*Nitrogen – Vacancy*) optical centers, which are found in diamond crystals doped with nitrogen. These optical centers form a system with discreet energy levels, whose properties to a great extent can be compared to the optical properties of isolated atoms. The particular value of NV optical centers lies in the fact that they reside in solid matter and thereby are more suitable for industrial applications in comparison with the atomic vapor. At the same time their severely discreet energy structure and the relatively low number of energy levels allow to describe them with methods used and well-tested working with the atoms in gaseous state.

Currently regular research group seminars are being organized to analyze the scientific literature about the research in NV centers implemented so far. The research laboratory where the experimental results will be obtained is also being planned by summarizing the information about the required equipment.

Publications

1. **Auzinsh, M., Ferber, R., Gahbauer, F., Jarmola, A., Kalvans, L., Papoyan, A., & Sarkisyan, D.** (2010). *Nonlinear magneto-optical resonances at D_1 excitation of ^{85}Rb and ^{87}Rb in an extremely thin cell*. Physical Review A, **81**, 033408. doi:10.1103/PhysRevA.81.033408
2. **Auzinsh, M., Ferber, R., Gahbauer, F., Jarmola, A., Kalvans, L., & Atvars, A.** (2011). *Cascade coherence transfer and magneto-optical resonances at 455 nm excitation of Cesium*. Optics Communications, **284**, 2863–2871. doi:10.1016/j.optcom.2011.01.088

3. **Auzinsh, M., Ferber, R., Fescenko, I., Kalvans, L., & Tamanis, M.** (2012). *Nonlinear magneto-optical resonances for systems with J∼100 observed in K$_2$ molecules*. Physical Review A, **85**, 013421. doi:10.1103/PhysRevA.85.013421

4. **Auzinsh, M., Berzins, A., Ferber, R., Gahbauer, F., Kalvans, L., Mozers, A., & Opalevs, D.** (2012). *Conversion of bright magneto-optical resonances into dark resonances at fixed laser frequency for D$_2$ excitation of atomic rubidium*. Physical Review A, **85**, 033418. doi:10.1103/PhysRevA.85.033418

5. **M.Auzinsh, A.Berzinsh, R.Ferber, F.Gahbauer, L.Kalvans, A.Mozers, A. Spiss.** (2012). *Enhancement of Level-Crossing Resonances by Frequency Control of the Exciting Radiation Field*, manuscript, unpublished.

Conference theses

C1. **I.Fescenko, M.Auzinsh, R.Ferber, L.Kalvans, M.Tamanis,***Studies of coherent population trapping in diatomic molecules*, 10th European conference on atoms molecules and photons ECAMP X, Spain, Salamanca, July 4-9, 2010

C2. **L. Kalvans, M. Auzinsh, A. Atvars, R. Ferber, F. Gahbauer, A. Jarmola,***Coherence transfer via cascades at caesium 7P$_{3/2}$ excitation*, 10th European Conference on Atoms Molecules and Photons ECAMP X, Spain, Salamanca, July 4-9, 2010

C3. **L. Kalvans, M. Auzinsh, R.Ferber, I. Fescenko, F.Gahbauer, A. Jarmola, A.Papoyan, D. Sarkisyan,***Magneto-optical resonances in atomic rubidium at D$_2$ excitation*, 10th European Conference on Atoms Molecules and Photons ECAMP X, Spain, Salamanca, July 4-9, 2010

C4. **L. Kalvāns**, *Sārmu metālu D1 ierosmē novērojamo tumšo magneto-optisko rezonanšu piesātināšanās*, LU 69. Konference, Rīga, 2011. gada februāris.

C5. **A. Bērziņš**, *^{85}Rb un ^{87}Rb nelineārās magneto-optiskās rezonanses pie D$_2$ ierosmes*, LU 69. Konference, Rīga, 2011. gada februāris.

C6. **A. Berzins, M. Auzinsh, R. Ferber, F. Gahbauer, L. Kalvans, A. Mozers, and D. Opalevs,***Influence of laser power density on bright and dark magneto-optical resonances*, 43rd Conference of the European Group for Atomic Systems (EGAS), University of Fribourg, Fribourg, Switzerland June 28 - July 2, 2011

C7. **Linards Kalvans, M. Auzinsh, A. Berzinsh, R. Ferber, F. Gahbauer, A. Mozers, D. Opalevs,***Conversion of dark magneto-optical resonances to bright by controlled changes in the excitation parameters of the Rb D$_2$ line at linearly polarized excitation*, Photonica 2011, Belgrade, Serbia August 29 – September 2, 2011

C8. **L.Kalvans, M.Auzinsh, A.Berzinsh, R.Ferber, F.Gahbauer, A.Mozers, A. Spiss,***Non-zero magnetic field level-crossing spectroscopy at D2 excitation of atomic Rubidium"*, V 'Rio de la Plata' Workshop on Laser Dynamics and Nonlinear Photonics, Colonia del Sacramento, Urugay, December 6 – 9, 2011

C9. **M. Auzinsh, A. Berzins, R. Ferber, F. Gahbauer, L. Kalvans, A. Mozers, and A. Spiss,***Level-crossing spectroscopy of atomic rubidium at D$_2$ excitation in the presence of a non zero magnetic field*, the 23rd International Conference on Atomic Physics ICAP 2012, Ecole Polytechnique, Palaiseau, France, July 23 – 27, 2012